Dev. Chem. Eng. Mineral Process., 11(3/4), pp. 363-380, 2003.

Production of Crystalline Boric Acid through the Reaction of Colemanite Particles with Propionic Acid

Bahman ZareNezhad
Dept of Chemical Engineering, Iran University of Science and Technology, P.O. Box 15875-4786, Tehran, Iran

A new process for boric acid production is developed. In this process the crystalline boric acid particles are directly produced in a one-stage crystallizer through the reaction of colemanite particles with propionic acid. Each porous colemanite particle is comprised of spherical solid grains. It is found that the solid boric acid produced precipitates on the unreacted core of the grains. The maximum overall conversion of colemanite particles can be increased to 97% if the propionic acid concentration, stirrer speed, colemanite mean particle size and temperature are set at 16 kmol/m^3, 20 Hz, 462 μm and 295 K, respectively. Therefore it is possible to use this process as an alternative for boric acid production, also having a useful side product. A particle-grain model is successfully used for process simulation.

Introduction

Applications of organic acids in the production of boric acid have been previously investigated (ZareNezhad et al., 1996). The reaction of borax particles with propionic acid solution to produce boric acid crystals follows a sharp interface-unreacted shrinking core model. However, reaction between borax solution and oxalic acid particles can be represented by a model for complete dissolution followed by precipitation (ZareNezhad, 1996).

In the industrial process of boric acid production from calcium borates, colemanite ($Ca_2B_6O_{11}.5H_2O$) is reacted with sulphuric acid and the by-product is $CaSO_4$ which gives rise to mineral blinding and environmental problems (Gerhartz, 1985). If propionic acid is used as the fluid reactant, the produced calcium propionate dissolves in the solution-phase and can be recovered as a useful side product. The reaction between colemanite particles and propionic acid solution can be written as:

$$Ca_2B_6O_{11}.5H_2O_{(S)} + 4\ C_2H_5COOH_{(L)} + 2\ H_2O \rightarrow 2\ Ca(C_2H_5COO)_2 + 6\ H_3BO_3 \qquad (1)$$

In this work, the production of boric acid through the reaction of colemanite particles with propionic acid solution is experimentally investigated and the mathematical modelling of the process based on a particle-grain approach is presented.

Experimental Procedures

The colemanite mineral used in the study was provided from three sources in the region of Emet, Kutahya, Turkey. After cleaning the mineral manually of visible impurities, it was ground and sieved by BS sieves to obtain the nominal particle size fractions of 462, 524, 780 and 840 μm. Sieving was repeated four times for each cut using a sieve shaker to obtain monosize colemanite particles. According to the microscopic observations, the shape of these particles were nearly spherical. Since the mineral was chosen specifically and cleaned mechanically, the purity of the crystals was very high. The chemical analysis of the colemanite crystals by a volumetric method (Jeffery et al., 1989) gave the following results: 27.35% CaO; 50.27% B_2O_3; 21.82% H_2O; 0.56% insoluble and other. These are in good agreement with stoichiometric values namely, 27.29% CaO; 50.81% B_2O_3 and 21.90% H_2O.

A micromeritics model 910 mercury intrusion porosimeter was used in this study to determine the pore size distribution of the colemanite particles. The instrument is capable of measuring pore sizes down to 2.5 nm. The values of porosities were checked by weight analysis of solid samples using a Sartorius balance (Model BP210D) having an accuracy of ± 0.01 mg.

A series of experiments were conducted in a 1.5 litre jacketed baffled cylindrical reactor maintained at a constant temperature within ±0.5 K. The stirrer was rotated by a variable speed stirrer motor (RZR-200, Heidolph), and the impeller speed set at the required values using a digital tachometer (Heidolph) attached to the motor. After charging the 1 litre propionic acid solution at a certain concentration into the reactor, the contents were heated to the required temperature. A given amount of the colemanite particles of a given mean size was added through a plastic funnel while the contents were stirred. The addition point was between the centre of the reactor and the vessel wall. Sampling was performed by pipetting about 5 ml of the contents from the reactor at different time intervals, and filtering it through a 0.4 μm pore size filter paper. The solid-phase samples were dissolved in HCl solution at 353 K and then analyzed for colemanite and boric acid. The calcium ion in the solution-phase was analyzed by a complexiometric method to check the accuracy of the analysis (Jeffery et al., 1989). Since the total amount of calcium in the solid and solution phases should remain constant, the accuracy of the analysis can be evaluated by:

$$\varepsilon_r = \frac{[(Ca_{slurry})_{n+1} + (Ca_{sample})_{n+1} - (Ca_{slurry})_n]}{(Ca_{slurry})_n} \times 100 \qquad (2)$$

The average error calculated as the mean of the absolute values of the errors was less than 1.2% for all runs. The arithmetic average of the results of the two experiments at each experimental condition was used in the kinetic analysis.

Samples of the solid phase were also analysed for crystal size distribution using the Coulter counter (Model Multisizer II). The solid samples collected on the filter paper were sieved using BS sieves to obtain two cuts of particle size fractions. A two-tube technique was employed to cover the wide size distribution of 8-900 μm. A 2000 μm orifice tube was used to analyse crystals with size range from 900 to 57 μm, and a 400 μm tube used for CSD measurement from 160 to 8 μm .

Initially a series of trial and error experiments was performed to determine the range of operating conditions to achieve the highest colemanite conversion. Subsequently a series of twenty experiments was carried out at different operating conditions. The parameters expected to influence the dissolution process were chosen as the acid concentration (c_o), stirrer speed (N), mean size of particle (L), and temperature (T). The process variables, their range and values are given in Table 1.

Table 1. *Ranges of operating conditions for the reaction of colemanite particles with propionic acid solution.*

Run	c_o (kmol/m^3)	N (Hz)	L (μm)	T (K)
T1-T5	10 - 16	21	462	288
T6-T10	12	18 - 34	462	288
T11-T15	12	20	462 - 780	288
T16-T20	16	20	462	288-308

Model Development

In this work it is assumed that a colemanite particle is initially comprised of uniformly-sized nonporous grains of spherical shape, each of which reacts in a shrinking core fashion (Levenspiel, 1998). As time progresses a layer of solid product builds up around the unreacted core of a grain. Owing to the differences in stoichiometric coefficients and in the molal density of the product and the reactant, the grains expand, resulting in a change in grain radius. These changes affect the particle porosity and hence the effective diffusivity. Figure 1 shows the geometry of the model.

The following assumptions are made for formulation of the problem:

1. The particles are monosize and spherical and the size of the particle does not change during the reaction. Since the expanded grains gradually fill the pores, the particle size remains nearly constant. Attrition of particle surface is neglected.
2. The grains retain their original spherical shape as they expand during the course of reaction.
3. First-order rate processes (film diffusion, pore diffusion, diffusion through the product layer, and chemical reaction) are assumed.
4. The reaction occurs at a sharp interface between the unreacted colemanite and the product boric acid in the grains. However with respect to the particle radius, reaction does not occur at a sharp boundary.

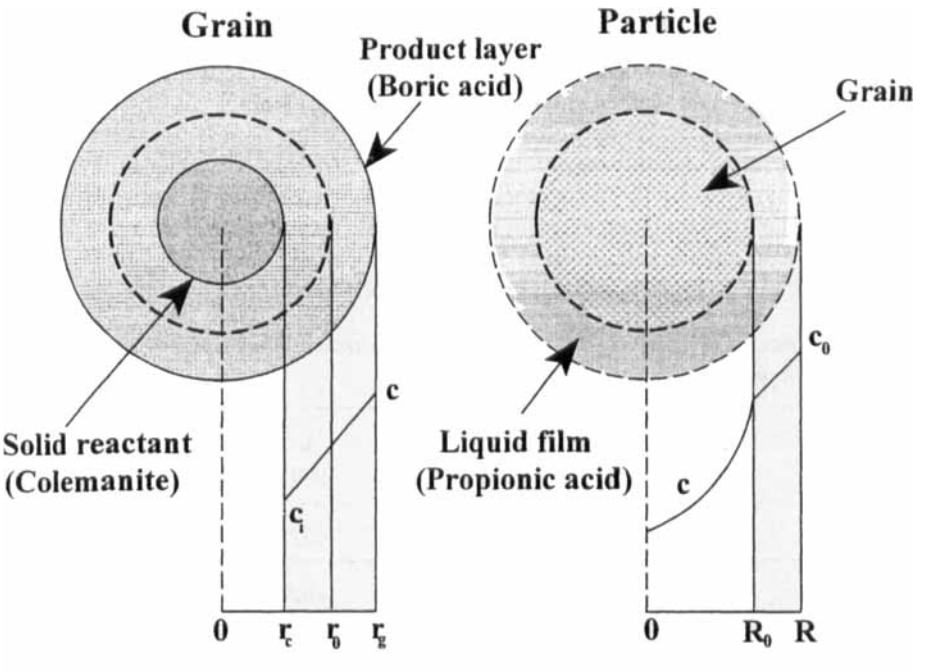

Figure 1. *Schematic representation of the proposed particle-grain model.*

(a) The Grain Model

In order to develop equations for the diffusion and reaction in the particle, it is first necessary to obtain the rate of reaction per grain. This is done by considering two series resistances, diffusion within the product layer (solid boric acid), and reaction at the surface of the unreacted-core of a grain. The molar rate of transport of propionic acid in each of these two steps can be written for a grain as follows:

(i) In the product layer, integration of the first-order diffusion rate equation for points of radius $r_c < r < r_g$ and concentration $c_i < c_g < c$ gives:

$$-\frac{dN_A}{dt}\left[\frac{1}{\eta_c}-\frac{1}{\eta_g}\right]=k_a A_{go}(c-c_i) \tag{3}$$

where N_A is the number of moles of propionic acid in the solution phase.

(ii) The chemical reaction at the surface of the unreacted-core of the grain:

$$-\frac{dN_A}{dt}\frac{1}{\eta_c^2} = k_s A_{g0} c_i \tag{4}$$

where $k_a = (D_p / r_0)$, $A_{g0} = 4\pi r_0^2$, $\eta_c = r_c / r_0$ and $\eta_g = r_g / r_0$

A mass balance for the conversion of solid reactant (colemanite) to the product layer (boric acid) can be written as:

$$\eta_g^3 - \eta_c^3 = Z(1 - \eta_c^3) \tag{5}$$

where:

$$\eta_c = (1 - x)^{1/3} \tag{6}$$

The parameter x is the grain conversion and Z is the volume of solid boric acid produced per unit volume of reacted solid colemanite (Sepulveda and Herbst, 1978) defined for this system as:

$$Z = \frac{6v_P}{v_B(1 - \varepsilon_P)} \tag{7}$$

where v_p and v_B are the molar volumes of the boric acid and colemanite respectively; and ε_p is the porosity of the solid boric acid.

A mass balance for the reaction between propionic acid and a colemanite grain can be written as:

$$-\frac{dN_A}{dt} = 4N_{g_0}\frac{dx}{dt} \tag{8}$$

where $N_{g0} = V_{g0} / v_B$. Combining Equations (3) to (8) gives:

$$\frac{dx}{dt} = \frac{v_B A_{g0}}{4V_{g0}} \frac{c k_s (1 - x)^{2/3}}{1 + \frac{k_s}{k_a}\left[(1 - x)^{1/3} - \frac{(1 - x)^{2/3}}{[1 + x(Z - 1)]^{1/3}}\right]} \tag{9}$$

(b) The Particle Model

Equation (8) gives the rate of reaction per grain. In order to determine the rate of disappearance of propionic acid (A) per unit volume of particle, we assume that the number of spherical grains per unit volume of particle at time zero, as given by $(1 - \varepsilon_0)/ V_{g0}$, is constant during the reaction. Therefore the rate of consumption of propionic acid per unit volume of particle is:

$$r_A = 4\frac{(1-\varepsilon_0)}{\nu_B}\frac{dx}{dt} \tag{10}$$

To allow for intraparticle concentration gradients, the mass conservation expression for propionic acid (A) within an element of spherical particle can be written assuming equimolar counter-diffusion and with the pseudo-steady state hypothesis (Luss, 1968):

$$\frac{1}{R^2}\frac{\partial}{\partial R}(R^2 D_e \frac{\partial c}{\partial R}) = r_A \tag{11}$$

where r_A is given by Equation (10). The boundary conditions for Equation (11) are:

$$\frac{\partial c}{\partial R} = 0 \quad \text{at} \quad R = 0 \tag{12}$$

$$D_e \frac{\partial c}{\partial R} = k_m (c_0 - c) \quad \text{at} \quad R = R_0 \tag{13}$$

Equations (12) and (13) are based on radial symmetry, and on an external boundary layer resistance expressed in terms of a liquid-film mass transfer coefficient.

The effect of structural changes on the effective diffusivity can be described by the random pore model of Wako and Smith (1963). According to this model the effective diffusivity of a fluid species through a monodisperse porous particle is:

$$D_e = D_A \frac{\varepsilon}{\gamma(\varepsilon)} = D_A \varepsilon^2 \tag{14}$$

where $\gamma(\varepsilon) = 1/\varepsilon$ and D_A is the bulk solution diffusion coefficient of that species (propionic acid). Equation (14) may be used to correlate changes in D_e due to changes in ε caused by grain expansion. Also the variation of particle porosity as a result of increase in grain size can be simply expressed in terms of the dimensionless grain radii, η_g, as:

$$\frac{1-\varepsilon}{1-\varepsilon_0}=(\frac{r_g}{r_0})^3=\eta_g^3 \tag{15}$$

Combining Equations (5), (6) and (15) gives a linear correlation between particle porosity and conversion as:

$$\varepsilon=\varepsilon_0-x(1-\varepsilon_0)(Z-1) \tag{16}$$

Thus the solution of the problem can be found by combining Equations (9) to (14) and Equation (16). In dimensionless form the governing equations are derived as:

$$\frac{1}{\eta^2}\frac{\partial}{\partial\eta}(D_e^*\eta^2\frac{\partial c^*}{\partial\eta})=\varphi^2\frac{dx}{d\tau} \tag{17}$$

where:

$$\frac{dx}{d\tau}=\frac{c^*(1-x)^{2/3}}{1+\beta\,[(1-x)^{1/3}-\frac{(1-x)^{2/3}}{[1+(Z-1)x]^{1/3}}]} \tag{18}$$

with boundary conditions:

$$\frac{\partial c^*}{\partial\eta}=0 \quad \text{at} \quad \eta=0 \tag{19}$$

$$\frac{\partial c^*}{\partial\eta}=\frac{Sh(1-c^*)}{D_e^*} \quad \text{at} \quad \eta=1 \tag{20}$$

and the initial condition:

$$x=0 \text{ at } \tau=0, \quad \text{for } 0\le\eta\le1 \tag{21}$$

where $\varphi = [(1-\varepsilon_0)\, k_s R_0^2 / r_0 D_{e0}]^{1/2}$, $\beta = k_s r_0 / D_p$, $Sh = k_m R_0 / D_{e0}$, $\tau = t / (4 r_0 / \nu_B k_s c_0)$, $c^* = c / c_0$, $D_e^* = D_e / D_{e0}$ and $\eta = R / R_0$.

Also the variation of effective diffusivity with particle porosity can be written in dimensionless form as:

$$D_e^* = \varepsilon^* \frac{\gamma(\varepsilon_0)}{\gamma(\varepsilon)} \tag{22}$$

Equation (16) can be written as the following dimensionless form, allowing for particle porosity change with conversion:

$$\varepsilon^* = 1 - \frac{(Z-1)(1-\varepsilon_0)\, x}{\varepsilon_0} \tag{23}$$

where $\gamma(\varepsilon) = 1/\varepsilon$ and $\varepsilon^* = \varepsilon / \varepsilon_0$. In order to complete the set of equations required for simulation of the process, the kinetic parameters, k_s and D_p should be determined. A fitting procedure is developed for estimating these parameters from experimental data as discussed in the next section.

Determination of the Kinetic Parameters

When pore diffusion and bulk diffusion effects can be neglected, the reaction rate constant can be directly estimated from the initial slope of the observed conversion versus time curve. In the reaction of colemanite particles with propionic acid solution, the influence of pore diffusion is found to be important. Therefore, a similar but more general procedure for determination of all kinetic parameters is presented in this section. Assuming that at the initial stage of the reaction no solid product layer is formed ($x = 0$ at $t = 0$), then an analytical solution of Equation (17) using the boundary conditions (Equations 19 and 20), can be obtained (Rice and Do, 1995) as:

$$c^* = \frac{\sinh(\varphi\eta)}{\eta \sinh\varphi\, [1 + (\varphi \coth\varphi - 1)/Sh]} \tag{24}$$

At $t = 0$, the molar rate of propionic acid consumption can be related to that of the particle as:

$$-N_{B0}\left(\frac{dX}{dt}\right)_{t=0} = -\frac{A_{ex}}{R_0} c_0 D_{e0} \left(\frac{dc^*}{d\eta}\right)_{\eta=1} \tag{25}$$

where $A_{ex} = 4\pi R_0^2$ and $N_{B0} = 4\pi R_0^3 (1 - \varepsilon_0)/ 3\nu_B$ for spherical particles. Combining Equations (24) and (25), the following equation can be derived at t = 0:

$$\left(\frac{dX}{dt}\right)_{t=0} = 3\frac{k_s \nu_B c_0}{r_0 \varphi^2}\left[\frac{\varphi \coth\varphi - 1}{1 + \frac{1}{Sh}(\varphi \coth\varphi - 1)}\right] \tag{26}$$

where $Sh = k_m R_0 / D_{e0}$ and $\varphi = [(1 - \varepsilon_0) k_s R_0^2 / r_0 D_{e0}]^{1/2}$. Thus the initial rate of overall conversion obtained from different trials can be used to estimate k_s. Since φ is a function of k_s, an iterative procedure using Newton-Raphson method was applied to obtain k_s from Equation (26) and using the experimental initial conversion rates. The bulk solution diffusivity (D_A) of propionic acid in water at different temperatures as estimated by the correlation of Wilke and Chang (1955), was combined with Equation (14) to calculate the value of D_{e0} (initial effective diffusivity of propionic acid through the particle). The solid-liquid mass transfer coefficient (k_m) was calculated by the correlation of Asai et al. (1986). Using scanning electron microscopy (SEM), the initial grain radius (r_0) was estimated to be about 0.2 μm. Having these initial estimates the trial and error calculation was carried out at each temperature until the following condition was satisfied:

$$\varepsilon_{k_s} = |[(dX/dt)_{t=0}]_{i,exp} - [(dX/dt)_{t=0}]_{i,calc})| < 10^{-4} \tag{27}$$

The best-fit value of k_s can be correlated in terms of an Arrhenius type expression:

$$k_s = k_{sr} \exp(-E_{ks}/RT) \tag{28}$$

Linear regression analysis of experimental data points in the form of ln k_s versus 1/T gives the values of the parameters k_{sr} and E_{ks}. The standard errors in the parameter estimates were determined at the 95% confidence limits, and are shown in Table 2. Substituting the calculated values of k_s in Equation (17), the value of D_p can be determined by using the single variable β (which is more convenient) as a fitting parameter, and simultaneous solution of Equations (17) to (23), for prediction of conversion-time dependence. It should be noted that the particle porosity (ε) does not disappear entirely, but attains a small residual value. Therefore in the present work ε_p (the limiting final porosity) is used as an added fitting parameter for fitting the data

over the full time span. This greatly improves the simulation results and prevents a too early cut-off of a conversion profile. The best-fit values of D_p are determined when the minimum deviations between predicted and experimental colemanite conversions are obtained. The objective function ε_{Dp} to be minimized is a relative mean square error defined as:

$$\varepsilon_{D_p} = \sqrt{\sum_{i=1}^{n} \frac{(\frac{X_{i,exp}}{X_{i,calc}} - 1)^2}{n}} \tag{29}$$

Thus the optimization is defined by minimizing the sum of square of the solid conversion residuals. The best fitted values of D_p (effective diffusivity of propionic acid through the solid boric acid layer) can be correlated in terms of an Arrhenius type expression:

$$D_p = k_{Dp} \exp(-E_{Dp}/RT) \tag{30}$$

Linear regression analysis of experimental data points in the form of ln D_p versus 1/T gives the values of the parameters k_{Dp} and E_{Dp}. The standard error in parameter estimates were determined at the 95% confidence limits, and are shown in Table 2. The best fit over the full time span was obtained at the limiting final porosity (ε_p) of 0.0207.

Table 2. *Values of the model parameters estimated from experimental data.*

Optimization results				
$k_{sr} \times 10^{-4}$ (m s^{-1})	$k_{Dp} \times 10^{9}$ (m s^{-1})	E_{ks} (kJ mol^{-1})	E_{Dp} (kJ mol^{-1})	$\varepsilon_p \times 10^2$
9.14 ± 0.21	3.46 ± 0.28	48.3 ± 0.17	26.4 ± 2.69	2.07 ± 0.23
$E_{ks} = 4.3 \times 10^{-5}$ $\varepsilon_{Dp} = 2.2 \times 10^{-3}$				

Simulation Algorithm

Equations (17) to (23), (28) and (30) were solved numerically using an orthogonal collocation technique based on the Legendre polynomials (Finlayson, 1972) to transform Equation (17) into a system of linear algebraic equations. Equation (18) was simultaneously integrated using a Runga-Kutta-Mersons method. For the range of parameters used, satisfactory convergence occurred with nine or less collocation

points. The overall conversion of colemanite particles at a given time was calculated from the following equation:

$$X = \frac{\int_0^V x\,dV}{\int_0^V dV} = 3\int_0^1 x\eta^2 d\eta \qquad (31)$$

Results and Discussion

Figure 2 shows a typical slice of a colemanite seed of mean size 780 μm used in run T15 comprising of very small spherical grains. In Figure 3, representing a partially reacted colemanite particle after 3000 seconds, expanded grains of about the same size covered with white precipitate (boric acid) are shown. The plugging of pore mouth occurs as a result of grain expansion.

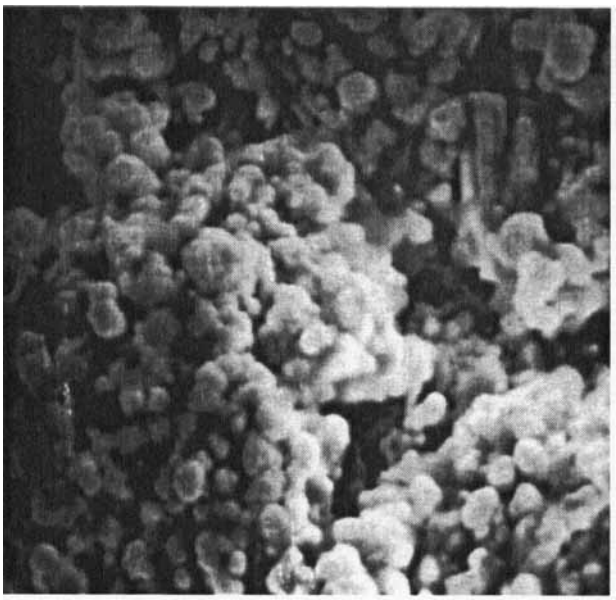

Figure 2. *A typical slice of a colemanite seed of size 780 μm (scale: 1 cm = 1 μm).*

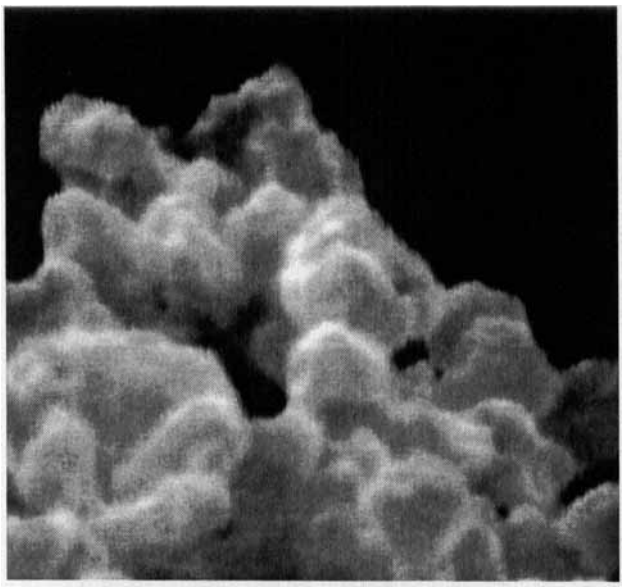

Figure 3. *A partially reacted colemanite particle after 3000 s (scale: 1 cm = 0.7 μm).*

The final undersize cumulative population of the crystals for three different colemanite particle sizes is shown in Figure 4. The distinctive curves obtained at the end of these runs clearly show that the final crystal size distributions are concentrated around the size of the feed particles. An increase from 2% to 5.5% in the % population of crystals with size less than 350 μm, as a result of increase in the size of colemanite particle from 462 to 780 μm, can be attributed to the higher rates of attrition of larger particles. Figure 4 shows that for the range of colemanite particle sizes used in this study, the majority of the total number of product crystals belongs to those crystals which have an average size around the size of colemanite seeds. Thus for model development, the surface attrition of particles is neglected and the particle sizes are assumed to be constant during the reaction.

The progressive changes in the pore size distribution of colemanite particles in a typical run are given in Figure 5 at different conversions. The initial pore size distribution shows that the pore sizes are mostly uniform and concentrated around 120 nm. Therefore, assuming that a colemanite particle is comprised of uniformly sized grains (shown previously) is shown to be justified. The value of the particle porosity

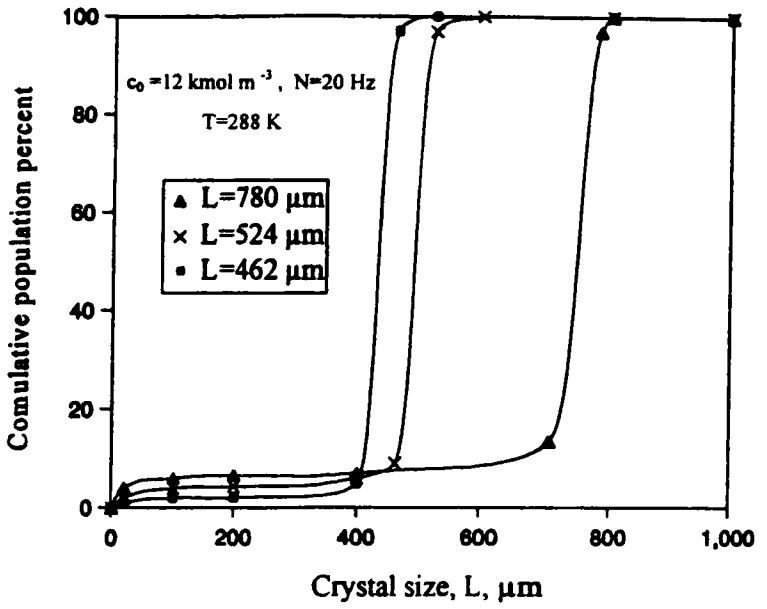

Figure 4. *Final crystal size distributions at different sizes of colemanite particles.*

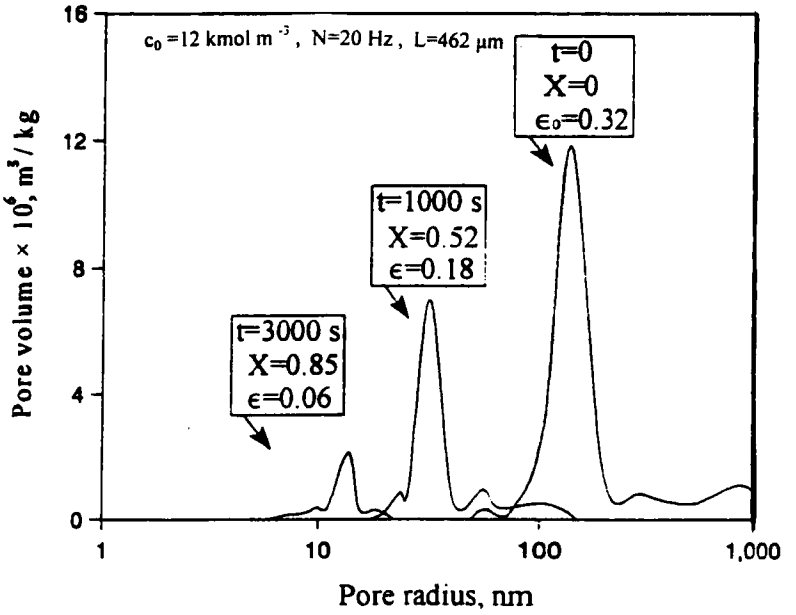

Figure 5. *Variations of pore size distribution of the particle during the reaction.*

obtained by mercury porosimetry is also shown at each conversion. The initial sharp peak around the initial average pore size shifts toward the smaller pore size indicating the gradual reduction of void volume as a result of boric acid deposition on the grains. Since the volume of produced boric acid crystals is about 1.52 times that of the reacted colemanite particles, a partial expansion of grains takes place when colemanite converts to solid boric acid. At higher solid conversion this phenomena may reduce the particle porosity to a very small value leading to pore plugging and thus maximum conversion. In this run 3000 seconds after commencing the dissolution process the conversion reaches its maximum value of X = 0.85, which from Figure 5 corresponds to a small porosity of the particle, $\varepsilon = 0.06$. Comparing this value with the initial porosity of the colemanite particle in this run, $\varepsilon_0 = 0.32$, then 81.3% reduction in the particle porosity is observed. This is consistent with the change of solid volume as the colemanite particles are converted to solid boric acid. .

The predicted and experimental conversion profiles for three different trials, all at L = 462 μm and different initial concentrations (c_0 from 10 to 16 kmol/m^3), are shown in Figure 6. Good agreement at higher propionic acid concentrations was obtained, while for lower fluid reactant concentrations the computed values are lower than the experimental results. At $c_0 = 10$ kmol/m^3, the predicted maximum conversion (87%) is 6.5% lower than the measured value (93%). All final conversions predicted by the proposed model are lower than the theoretical maximum conversion (99%) evaluated by Equation (16), demonstrating the effect of intraparticle diffusional resistance.

The predicted and measured colemanite conversions of three trials at different sizes of colemanite particles are compared in Figure 7. Good agreement between model and experiment was achieved for the smaller particles. The dissolution process proceeds rapidly in its early stages but slows down as the time of reaction continues, and the major portion of boric acid is produced during the first 1000 seconds. It should be noted that the predicted conversion profiles would be qualitatively different if the model did not account for changes of D_e with time. In fact at L = 462 μm, the model would predict 100% conversion within 1500 seconds if changes in D_e were ignored. The simulation results indicate that as the size of colemanite particles is increased from 462 to 780 μm, the maximum attainable conversion decreased from 91% to 66%, showing the increasing influence of intraparticle diffusion as the particle size is increased. The larger deviation between simulated and measured conversions for larger particles (i.e. 780 μm) can be attributed to increasing rate of attrition as a result of increase in particle size.

Model predictions are compared with experimental data at three different temperatures in Figure 8. An initial increase in reaction rate may occur as reaction temperature is increased, but with the associated increase in the diffusional resistance, rapid pore closure may decrease the reaction rate. The experimental data show that as the reaction temperature is increased from 288 to 295 K, the maximum colemanite conversion is increased from 93% to 97%, while a further increase in temperature from 295 to 308 K results in a decrease in the conversion after 2000 seconds and thus a lower maximum conversion of 93% is obtained. In the temperature ranges used in this study, the simulated results are in relatively good agreement with experimental data.

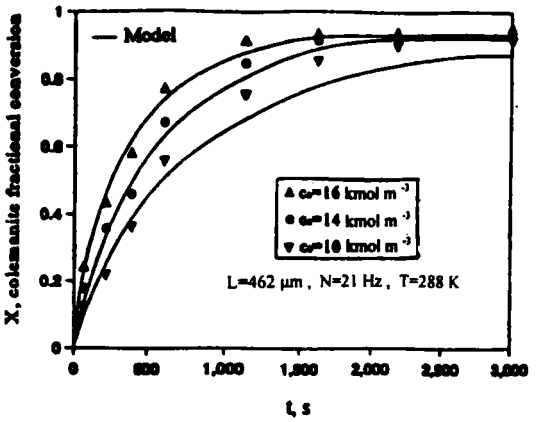

Figure 6. *Simulated and measured colemanite conversion at different acid concentrations.*

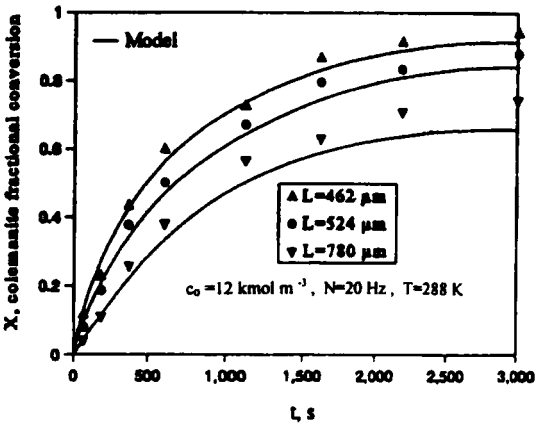

Figure 7. *Simulated and measured colemanite conversion at different sizes of colemanite particles.*

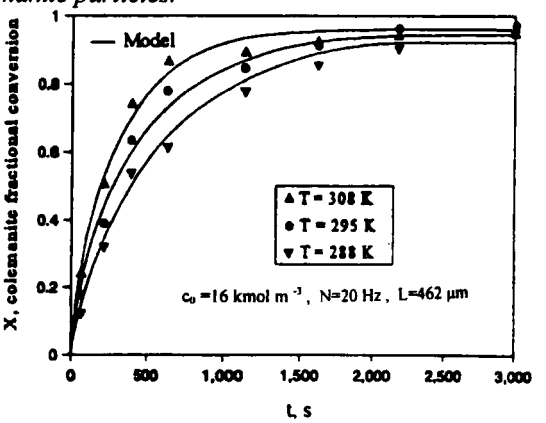

Figure 8. *Simulated and measured colemanite conversion at different temperatures.*

Conclusions

In the reaction between colemanite particles and propionic acid solution, the boric acid product precipitates in the porous matrix of the particle. The gradual reduction in colemanite particle porosity and the existence of a maximum limiting conversion observed in all experiments suggests the significance of a pore diffusion step in this process. The maximum conversion can be increased by using smaller colemanite particles, and/or increasing the solution temperature. For the range of process variables used in this study, the maximum colemanite conversion can be increased to 97% if the propionic acid concentration, stirrer speed, colemanite particle size and temperature are set at 16 kmol/m^3, 20 Hz, 462 μm and 295 K, respectively. Therefore, it is possible to use this process as an alternative for boric acid production which also has a useful by-product. A model based on the particle-grain approach is presented for predicting the conversion profiles of colemanite particles during the reaction. It is assumed that the product boric acid is deposited on the expanding spherical grains, leading to a gradual particle porosity reduction. A method for simultaneous determination of the kinetic parameters was developed. Although there are some discrepancies between the model and experimental measurements, generally the trend of the simulation results is in agreement with observed values. Overall, the proposed model is more accurate at higher acid concentrations, lower stirrer speed and smaller colemanite particle sizes for which the attrition rate is lower. According to the model, the chemical reaction, the pore diffusion and product layer resistances are important influencing steps in the production of crystalline boric acid through the reaction of colemanite particles with propionic acid solution.

Nomenclature

A_{ex}	External surface of a particle	(m^2)
A_{g0}	Initial external surface of a grain	(m^2)
c	Propionic acid concentration at the grain surface	(kmol m^{-3})
c_i	Propionic acid conc. at the core surface	(kmol m^{-3})
c_0	Propionic acid conc. in the solution	(kmol m^{-3})
c^*	Normalized propionic acid conc. in the solution	
$(Ca_{slurry})_{n+1}$	Calcium in the solution after $(n+1)^{th}$ sampling	(kmol)
$(Ca_{sample})_{n+1}$	Calcium in the $(n+1)^{th}$ sampling	(kmol)
$(Ca_{slurry})_n$	Calcium in the solution before $(n+1)^{th}$ sampling	(kmol)
D_A	Diffusion coefficient of propionic acid in the solution	(m^2 s^{-1})
D_p	Product layer diffusion coefficient	(m^2 s^{-1})
D_e	Effective diffusivity of acid through the particle	(m^2 s^{-1})
D_{e0}	Initial effective diffusivity through the particle	(m^2 s^{-1})
D_e^*	Normalized effective diffusivity through the particle	
E_{ks}	Activation energy of chemical reaction	(kJ mol^{-1})
E_{Dp}	Activation energy of diffusion through the product	(kJ mol^{-1})
i	Data point i	
k_a	Rate constant of diffusion through the product layer	(ms^{-1})

k_m	Solid-liquid mass transfer coefficient	(ms^{-1})
k_s	Reaction rate constant	(ms^{-1})
k_{sr}	Parameter defined in Equation (28)	(ms^{-1})
k_{Dp}	Parameter defined in Equation (30)	(ms^{-1})
L	Particle size	(m)
N	Stirrer speed	(Hz)
N_A	Moles of propionic acid in the solution phase	(kmol)
N_{g0}	Initial number of moles of colemanite in a grain	(kmol)
N_{B0}	Initial number of moles of colemanite in a particle	(kmol)
n	Number of data points	
R	Gas constant (= 8.314)	$(J\ mol^{-1}K^{-1})$
R_0	Radius of a particle	(m)
r_0	Initial grain radius	(m)
r_c	Radius of unreacted core of a grain	(m)
r_g	Grain radius	(m)
r_A	Consumption rate of acid per unit particle volume	$(kmol^{-3}\ s^{-1})$
Sh	Sherwood number	
T	Temperature	(K)
t	Time	(s)
V_{g0}	Initial grain volume	(m^3)
V	Particle volume at a given radius	(m^3)
X	Fractional conversion of colemanite particles	
$X_{i,exp}$	Experimental colemanite conversion at data point i	
$X_{i,calc}$	Calculated colemanite conversion at data point i	
x	Grain conversion	
Z	Volume of solid boric acid per unit volume of solid colemanite	

Greek symbols

β	Dimensionless parameter used in Equation (18)	
η_c	Normalized radius of unreacted core of a grain	
η_g	Normalized grain radius	
η	Normalized particle radius	
ν_B	Molar volume of solid colemanite	$(m^3\ (kmol)^{-1})$
ν_p	Molar volume of solid boric acid	$(m^3\ (kmol)^{-1})$
ε_p	Final porosity	
ε_0	Initial porosity of the colemanite particle	
ε	Porosity of the colemanite particle at time t	
ε^*	Normalized particle porosity	
ε_{ks}	Error parameter defined in Equation (27)	(s^{-1})
ε_{Dp}	Error parameter defined in Equation (29)	
ε_r	Error parameter defined in Equation (2)	
$\gamma(\varepsilon)$	Parameter defined in Equation (14)	
φ	Normalized modulus defined in Equation (17)	
τ	Normalized time	

References

Asai, S., Konishi, Y., and Sasaki, Y. 1986. Mass transfer between fine particles and liquids in an agitated vessel. *Third World Congress of Chemical Engineering*, Tokyo, Japan, Part **II**, 428-430.

Finlayson, B. 1972. The Method of Weighted Residuals and Variational Principles, pp.86-99, Academic Press, London.

Gerhartz, W. 1985. Ullmann's Encyclopedia of Industrial Chemistry, **I**, 123-136, Berlin, Germany.

Jeffery, G.H., Bassett, J., Mendham, J., and Denney, R.C. 1989. Vogel's Textbook of Quantitative Chemical Analysis, 5th Edition, Chapter 5, pp.202-221, Longman Group, UK.

Levenspiel, O. 1998. Chemical Reaction Engineering, 3rd Edition, pp.234-250, Wiley & Sons, Inc., New York.

Luss, S. 1968. Reaction and diffusion in porous media. *Can. J. Chem. Eng.*, **46**, 154-159.

Rice, R., and Do. J. 1995. Applied Mathematics and Modelling for Chemical Engineers, pp.108-132, McGraw-Hill, New York.

Sepulveda, J.E., and Herbst, J.A. 1978. Reaction in multiparticle sysytems. AIChE. Symposium Series, **74**(173), pp.41-65.

Wako, N.. and Smith, J.M. 1963. Diffusion in catalyst pellets. *Chem. Eng. Sci.*, **17**, 825-834.

Wilke, C.R.. and Chang, P. 1955. Predicting the bulk diffusion coefficient of a species in the solution phase. *AIChE J.*, **1**, 264-268.

ZareNezhad, B. 1996. Crystal size distribution control in reactive precipitation processes. *Dev. Chem. Eng. Mineral Process.*, **4**(3), 213-222.

ZareNezhad, B., Manteghian, M., and Tavare, N.S. 1996. On the confluence of dissolution, reaction and precipitation. *Chem. Eng. Sci.*, **51**(11), 2547-2552.

Received: 25 February 2002; *Accepted after revision:* 1 October 2002.